MOLECULAR AND CELLULAR BIOLOGY, Dec. 2011, p. 4775–4788 Vol. 31, No. 23
0270-7306/11/$12.00 doi:10.1128/MCB.05646-11

Survival and Differentiation of Mammary Epithelial Cells in Mammary Gland Development Require Nuclear Retention of Id2 Due to RANK Signaling▽

Nam-Shik Kim,[1,2] Hyoung-Tai Kim,[1] Min-Chul Kwon,[1] Suk-Won Choi,[1] Yoon-Young Kim,[2] Ki-Jun Yoon,[1] Bon-Kyoung Koo,[1] Myung-Phil Kong,[2] Juhee Shin,[2] Yunje Cho,[2] and Young-Yun Kong[1]*

Department of Biological Sciences, Seoul National University, San 56-1, Silim-Dong, Gwanak-Gu, Seoul 151-747, South Korea,[1] *and Department of Life Science, POSTECH, Pohang, Kyungbuk 790-784, South Korea*[2]

Received 17 May 2011/Returned for modification 9 July 2011/Accepted 19 September 2011

RANKL plays an essential role in mammary gland development during pregnancy. However, the molecular mechanism by which RANK signaling leads to mammary gland development is largely unknown. We report here that RANKL stimulation induces phosphorylation of Id2 at serine 5, which leads to nuclear retention of Id2. In lactating *Id2*Tg; *RANKL*$^{-/-}$ mice, Id2 was not phosphorylated and was localized in the cytoplasm. In addition, in lactating *Id2*^{S5A}Tg mice, Id2^{S5A} (with serine 5 mutated to alanine) was exclusively localized in the cytoplasm of mammary epithelial cells (MECs), while endogenous Id2 was localized in the nucleus. Intriguingly, nuclear expression of Id2^{S5A} rescued increased apoptosis and defective differentiation of MECs in *RANKL*$^{-/-}$ mice. Our results demonstrate that nuclear retention of Id2 due to RANK signaling plays a decisive role in the survival and differentiation of MECs during mammary gland development.

The mammary gland is a complex organ that proliferates and differentiates during puberty, pregnancy, and lactation under the influence of various hormones, including estrogen, progesterone, and prolactin. At birth, the mammary anlage consists of a few rudimentary ducts that occupy a small portion of the mammary fat pad. Pronounced ductal elongation and side branching commence at puberty. During pregnancy, the complexity of the ductal system increases through the addition of side branches, the formation of lobuloalveolar structures, and the differentiation of secretory epithelia (5, 13, 14). These proliferation, survival, and lactogenic differentiation steps are essential to form a functional lactating mammary gland during pregnancy.

RANKL, a key regulator of osteoclast differentiation and/or activation (1, 16, 20, 22), is essential for the development of a lactating mammary gland during pregnancy (10) and for the expansion of adult mammary stem cells (MaSC) in normal development (2, 17) and breast cancer (11, 36). Mice lacking RANKL or its receptor, RANK, showed impaired lobuloalveolar development during pregnancy, owing to intrinsic defects in the proliferation, survival, and lactogenic differentiation of mammary epithelial cells (MECs). Recent studies have reported that both progesterone (6, 31) and prolactin (40) signaling induce the expression of RANKL, and progesterone induces the expansion of MaSC by a paracrine effecter, RANKL, suggesting that these hormones regulate mammary gland development via the RANKL-RANK signaling pathway (2, 11, 17, 36). However, how RANKL-RANK signaling regulates various aspects of the proliferation, survival, and differentiation of MECs in lactating mammary gland development needs to be elucidated. Cao et al. suggested that activation of a linear RANK–IκB kinase α (IKKα)–NF-κB–cyclin D1 signaling cascade could lead to the cellular proliferation of MECs (7). Although we suggested that RANK signaling induces β-*casein* gene expression via CCAAT/enhancer-binding protein β (C/EBPβ) (18), the molecular mechanisms of RANK signaling resulting in the survival and lactogenic differentiation of MECs need to be determined.

Id proteins, inhibitors of DNA binding/differentiation, lack a DNA-binding domain but possess a helix-loop-helix motif and hence can inhibit the function of bHLH transcription factors in a dominant-negative manner by suppressing their heterodimerization partners (32). Similar to RANKL-deficient mice, Id2-deficient mice display impaired lobuloalveolar development during pregnancy and intrinsic defects in cell proliferation, survival, and lactogenic differentiation (28, 30). We previously reported that RANKL-RANK signaling induces the nuclear translocation of Id2 in MECs (19), and Kurooka and Yokota reported that Id2 possesses a nuclear export sequence and is actively transported from the nucleus into the cytoplasm via a CRM1/exportin-dependent pathway (21). Because nucleocytoplasmic shuttling serves to regulate the functions of many signaling molecules and transcriptional factors (8, 9, 39), we speculated that the nuclear localization of Id2 by RANK signaling might be important for lactating mammary gland development.

In the present study, we found that serine 5 (Ser-5) of Id2 is phosphorylated by RANKL stimulation via the phosphatidylinositol 3-kinase (PI3K)–p38 mitogen-activated protein kinase (MAPK)–cyclin-dependent kinase 2 (Cdk2) signaling pathway. The phosphorylation of Id2 at Ser-5 prevented CRM1/exportin-dependent nuclear export, which results in the nuclear re-

* Corresponding author. Mailing address: Department of Biological Sciences, Seoul National University, San 56-1, Silim-Dong, Gwanak-Gu, Seoul 151-747, South Korea. Phone: 82-2-880-2638. Fax: 82-2-872-1993. E-mail: ykong@snu.ac.kr.

▽ Published ahead of print on 26 September 2011.

tention of Id2. To determine whether Id2 needs to be localized in the nucleus for lactating mammary gland development, we generated transgenic (Tg) lines that express wild-type Id2, mutant Id2^{S5A} (Ser-5 of Id2 was mutated to an alanine, which is not phosphorylated by RANK signaling), or nuclear localization sequence (NLS)-tagged mutant Id2^{S5A} under the control of the mouse mammary tumor virus (MMTV) promoter: MMTV-*Id2* (*Id2*Tg), MMTV-*Id2*^{S5A} (*Id2*^{S5A}Tg), and MMTV-*NLS-Id2*^{S5A} (*NLS-Id2*^{S5A}Tg) mice, respectively. Mutant Id2^{S5A} was exclusively localized in the cytoplasm of MECs from *Id2*^{S5A}Tg mice, while endogenous Id2 was localized in the nucleus, demonstrating that the Ser-5 phosphorylation of Id2 by RANK signaling is required for its nuclear retention. When *Id2*Tg mice were bred to *RANKL*$^{-/-}$ mice, exogenous Id2 was localized in the cytoplasm, and the mammary gland defects of *RANKL*$^{-/-}$ mice were not rescued. In the *NLS-Id2*^{S5A}Tg; *RANKL*$^{-/-}$ mice, however, the increased apoptosis and defective differentiation observed in *RANKL*$^{-/-}$ mice were rescued, while defective cellular proliferation was not. Furthermore, nuclear expression of NLS-Id2^{S5A} in virgin mice induced the expression of milk genes and the cellular differentiation of MECs. These results demonstrate that RANK signaling prevents nuclear export of Id2 by Cdk2-dependent phosphorylation of Ser-5, which allows Id2 to remain in the nucleus and function as a key downstream mediator of RANK signaling in lactating mammary gland development by inhibiting apoptosis and inducing differentiation in MECs.

MATERIALS AND METHODS

Mice. To obtain transgenic vectors, 0.5-kb HindIII/XbaI fragments from the plasmids pcDNA3.0-murine Id2, -murine Id2^{S5A} (a mutant created by replacing Ser-5 with alanine), and -murine NLS-Id2^{S5A} vectors (19) were ligated into the MMTV long terminal repeat (LTR) plasmid, which directs expression chiefly to the mammary epithelium (34, 38). The inserts from the transgenic vectors, pMMTV-Id2, -Id2^{S5A}, and -NLS-Id2^{S5A}, were microinjected into the pronuclei of fertilized one-cell zygotes from FVB/N mice. The offspring were identified by Southern blot screening of EcoRI-digested genomic DNA. Further genotyping was performed by PCR of tail biopsy specimens. Mice genetically deficient for *RANKL* or *Id2* have been described previously (20, 43). *Id2*Tg; *RANKL*$^{-/-}$, *Id2*Tg; *Id2*$^{-/-}$, *NLS-Id2*^{S5A}Tg; *RANKL*$^{-/-}$, and *NLS-Id2*^{S5A}Tg; *Id2*$^{-/-}$ mice were generated by mating the *Id2* or *NLS-Id2*^{S5A} transgenic females with *RANKL*$^{-/-}$ or *Id2*$^{-/-}$ males. A strain of the mice, *Id2*Tg; *RANKL*$^{-/-}$, *Id2*Tg; *Id2*$^{-/-}$, *NLS-Id2*^{S5A}Tg; *RANKL*$^{-/-}$, and *NLS-Id2*^{S5A}Tg; *Id2*$^{-/-}$ mice, is FVB/N over N6 generation of backcross with FVB/N. All mice were maintained at the animal facilities of POSTECH and Seoul National University.

MCF7 cell lines. Murine stem cell virus (MSCV)-HA-Id2-ER-MCF7 cells and MSCV-HA-Id2^{S5A}-ER-MCF7 cells were generated by transducing MCF7 cells with an MSCV-puro retroviral vector engineered to express hemagglutinin (HA)-Id2-estrogen receptor (ER) or HA-Id2^{S5A}-ER, respectively.

Immunohistochemistry and immunocytochemistry. Histological analyses were performed as described previously (19). Sections (4 μm) were stained with the following antibodies: rabbit anti-Id2 (1:100; Santa Cruz Biotechnology), rabbit anti-active-caspase 3 (1:300; BD Biosciences), rabbit anti-NKCC1 (1:200; a generous gift from R. James Turner, NIH/NIDCR), mouse anti-HA (1:300; Santa Cruz Biotechnology), and mouse anti-smooth muscle actin (anti-SMA) (1:200; Neomarker). For bromodeoxyuridine (BrdU) labeling, mice were injected with BrdU (50 μg/g of body weight) 3 h before sacrifice. BrdU incorporation was assessed with a mouse anti-BrdU antibody (1:1,000; BD Biosciences). Specific binding was detected with Alexa 488- or Alexa 594-labeled secondary antibodies (Molecular Probes). Fixed cells were incubated in blocking solution (3% bovine serum albumin [BSA], 3% goat serum, and 0.5% Tween 20 in phosphate-buffered saline [PBS]) at room temperature for 4 h, followed by additional incubation with an anti-HA antibody (1:300; Santa Cruz Biotechnology). Subsequently, the cells were stained with Alexa 488-labeled anti-mouse IgG (Molecular Probes) at room temperature for 1 h.

HA-Id2-ER- and HA-Id2^{S5A}-ER-expressing MCF7 cells were incubated for 6 h in Dulbecco's modified Eagle's medium (DMEM) containing 10% fetal bovine serum (FBS) and 4-hydroxytamoxifen (4-OHT) (Sigma; catalog no. H7904; 1 μM) and then were pretreated with kinase inhibitors—Cdk2 inhibitor II (Calbiochem; catalog no. 219445; 15 μM), roscovitine (Calbiochem; catalog no. 557360; 15 μM), p38 MAPK inhibitor (SB203580; Calbiochem, catalog no. 559389; 30 μM), PI3K inhibitor (LY294002; Calbiochem; catalog no. 440202; 20 μM), and c-Jun N-terminal kinase (JNK) inhibitor (Calbiochem; catalog no. 420119; 25 μM)—for 3 h prior to RANKL (PeproTech; catalog no. 315-11; 100 ng/ml) stimulation for 3 h. The cells were then fixed with 4% paraformaldehyde at room temperature for 15 min. The fixed cells were incubated in blocking solution (3% bovine serum albumin, 3% goat serum, and 0.5% Tween 20 in PBS) at room temperature for 4 h, followed by an additional incubation with anti-HA antibody (1:300; Santa Cruz Biotechnology). Subsequently, the cells were stained with Alexa 594-labeled anti-mouse IgG (Molecular Probes) at room temperature for 1 h. Images were taken using a Zeiss Axioskop2 Plus microscope and a Zeiss LSM510 confocal microscope.

Quantification of nuclear and cytoplasmic fluorescence. Fluorescence in the nucleus or cytoplasm was quantified using the ImagePro Plus program. Pixel intensity readings were taken from either the nucleus or the cytoplasm of over 80 cells. Values were averaged for each group, representative of three independent experiments. Nuclear fluorescence was then normalized to cytoplasmic fluorescence by dividing the average nuclear pixel intensity by the average cytoplasmic pixel intensity from each group.

Immunoblotting. MCF7 cells were transfected with 4 μg of plasmid DNA per 10-cm plate and then resuspended in immunoprecipitation (IP) buffer (120 mM HEPES-NaOH [pH 7.5], 3 mM EDTA, 3 mM $CaCl_2$, 80 mM NaCl, 1% Triton X-100, 5 mM dithiothreitol). For immunoblotting, equal amounts of whole-cell extracts were separated on SDS-PAGE and transferred to polyvinylidene difluoride (PVDF) membranes. The membranes were incubated with antibodies to Id2 (Santa Cruz Biotechnology), HA (Santa Cruz Biotechnology), p-Id2(Ser-5), p-Akt (Cell Signaling), Akt (Cell Signaling), p-p38 MAPK (Cell Signaling), p38 MAPK (Cell Signaling), p-Cdk2 (Cell Signaling), Cdk2 (Santa Cruz Biotechnology), and E-cadherin (BD Biosciences), followed by a goat anti-rabbit or an anti-mouse horseradish peroxidase-conjugated secondary antibody (Promega). The band intensities of Western blots were quantified using the NIH Image J program. Pixel intensity readings were taken from either the HA or p-Id2 Ser-5 band.

Quantitative real-time RT-PCR. For quantitative real-time reverse transcription (RT)-PCR, total RNA was extracted from the isolated mammary tissues with TRIzol reagent (Sigma) according to the manufacturer's instructions. Aliquots of 1 or 2 μg RNA were used for reverse transcription (Promega) with oligo(dT) priming. Real-time PCRs were set up with 1/25 of each cDNA preparation in an Applied Biosystems 7300 real-time PCR system with a master mix of SYBR green I premix ExTaq (Takara Bio) according to the manufacturer's instructions Relative expression levels and statistical significance were calculated based on a cytokeranin 18 (CK18) standard, using LightCycler software. The sequences of the synthesized oligonucleotides were as follows: CK18-F, 5′-GGGCCACTACTTCAAGATCA-3′, and CK18-R, 5′-GGTGTCATCTACCACCTTGC-3′; β-casein-F, 5′-AAGCTAAAGCCACCATCCTT-3′, and β-casein-R, 5′-CAGCTGGGTCTGAGAAGAAA-3′; Wap-F, 5′-TGAGGGCACAGAGTGTATCA-3′, and Wap-R, 5′-TCGCTGGAGCATTCTATCTT-3′; α-lactoalbumin-F, 5′-TGAATGGGCCTGTGTTTTAT-3′, and α-lactoalbumin-R, 5′-CACGCTATGTCATCATCCAA-3′; Id2-F, 5′-TTAGGAAAAACAGCCTGTCG-3′, and Id2-R, 5′-GCAGGTCCAAGATGTAATCG-3′; RANKL-F, 5′-CCCTGATGAAAGGAGGAAGC-3′, and RANKL-R, 5′-TGGAGACCTCGATGCTGATT-3′; β-actin-F, 5′-TCATGAAGTGTGACGTTGACATCCGT-3′, and β-actin-R, 5′-CCTAGAAGCATTTGCGGTGCACGATG-3′; Bcl-2-F, 5′-ACTTCGCAGAGATGTCCAGTC-3′, and Bcl-2-R, 5′-TGGCAAAGCGTCCCCTC-3′; Bcl-X_L-F, 5′-GAATGGAGCCACTGGCCA-3′, and Bcl-X_L-R, 5′-GCTGCCATGGGAATCACCT-3′.

Production of antibody specific for phosphorylated Ser-5 of Id2. A 10-mer synthetic peptide containing N-terminal residues 1 to 10 of Id2 that mimicked phosphorylation of Ser-5 was injected into rabbits, followed by boosts at 14, 28, and 42 days. Anti-phospho-Id2 antiserum was obtained at day 49 and purified by affinity purification over a phospho-Id2 column (Affi-Gel; Bio-Rad). The specificity of the purified anti-phospho-Id2 antiserum was assessed by Western blotting using lysates from MCF7 cells expressing wild-type Id2 or Id2^{S5A} (a mutant created by replacing Ser-5 with alanine).

RESULTS

Id2 phosphorylation by RANK signaling prevents its nuclear export. We reported previously that Cdk2 might be im-

portant for the RANKL-induced nuclear localization of Id2 in MECs (19), and Ser-5 of Id2 has been suggested to be a functional phosphorylation site for Cdk2 (12). However, whether RANKL stimulation indeed results in the phosphorylation of Id2 and whether phosphorylation is required for nuclear localization of Id2 have not been evaluated. To address these issues, we generated the two fusion proteins HA-Id2-ER and HA-Id2^{S5A}-ER by fusing Id2 and Id2^{S5A}, respectively, with the carboxyl terminus of the murine ER (15). We then established Id2-ER or Id2^{S5A}-ER-expressing MCF7 stable cell lines. Moreover, we generated specific antibody for phospho-Ser-5 of Id2. We could detect specific signal for p-Id2 (Ser-5) only in HA-Id2-expressing MCF7 cell lysates and decrease of the signal by Cdk2 inhibitor II (Fig. 1A).

To test whether RANKL stimulation can phosphorylate Ser-5 of Id2 via Cdk2, Id2-ER-expressing MCF7 cells were treated with RANKL in the presence of 4-OHT. As expected, phosphorylation of Ser-5 of Id2 was readily enhanced by RANKL stimulation and inhibited by Cdk2 inhibitors, Cdk2 inhibitor II and roscovitine (the inhibitor of Cdks [Cdk1, -2, -5, -7, and -9]) (Fig. 1B). Because MCF7 cells express both RANKL and its receptor (16), a substantial basal level of Id2 phosphorylation might be due to RANK signaling induced by the endogenously expressed RANKL in MCF7 cells (Fig. 1B). Indeed, Id2 phosphorylation was decreased by treating the MCF7 cells with *RANKL* small interfering RNA (siRNA) (Fig. 1C and D). These results show that RANKL stimulation induces the phosphorylation of Ser-5 of Id2 via Cdk2.

We next examined whether nuclear localization of Id2 requires phosphorylation of Ser-5. In our previous study, we found that RANKL stimulation resulted in nuclear localization of HA-Id2 overexpressed in HC11 and MCF7 cells and mouse primary MECs. However, HA-Id2 was also substantially localized (9.3%, 8.0%, and 12.8% in HC11 and MCF7 cells and primary MECs, respectively) in the nucleus even without RANKL stimulation (19). To clearly verify that RANKL induced Id2 localization, we utilized the Id2-ER and Id2^{S5A}-ER constructs in this study. Because both ER and Id2 have nuclear export sequences (21, 26), both Id2-ER and Id2^{S5A}-ER were retained in the cytoplasm in the absence of 4-OHT (Fig. 1E). However, most of the Id2-ER was localized in the nucleus by 4-OHT treatment, which was inhibited by *RANKL* siRNA treatment (Fig. 1E and F). Consistently, mutant Id2^{S5A}-ER was promptly exported to the cytoplasm (Fig. 1E and F). Prompt export of *RANKL* siRNA-treated Id2 and Id2^{S5A} is due to CRM1/exportin-dependent nuclear export, because 4-OHT treatment with LMB, an inhibitor of CRM1/exportin-dependent nuclear export, resulted in the complete accumulation of both *RANKL* siRNA-treated Id2 and Id2^{S5A} in the nucleus (Fig. 1E and F). The nuclear localization of Id2 was inhibited by Cdk2i (Cdk2), LY294002 (PI3K), and SB203580 (p38 MAPK), but not by IKK inhibitor, JNK inhibitor, and PD98059 (Erk) (Fig. 1G and H); this suggests that the PI3K- and p38 MAPK-dependent pathways might be involved in the nuclear localization of Id2 by RANKL stimulation.

Consistently, RANKL stimulation induced the phosphorylation of Akt and p38 MAPK, which preceded the phosphorylation of Cdk2 (Fig. 1I). Indeed, the phosphorylation of Cdk2 at the activating threonine 160 was blocked by the LY294002 (PI3K) and SB203580 (p38 MAPK) pathway inhibitors (Fig. 1J), indicating that both Akt and p38 MAPK act upstream of Cdk2. However, the phosphorylation of Akt and p38 MAPK was inhibited by both PI3K and p38 MAPK inhibitors (Fig. 1I), which is consistent with a previous report that Akt physically associates with the p38 MAPK complex and that they can phosphorylate each other in human neutrophils (33). Indeed, the association between Akt and p38 MAPK was increased by RANKL stimulation (Fig. 1K). Taken together, our results suggest that Akt-p38 MAPK-Cdk2-mediated phosphorylation of Ser-5 of Id2 after RANKL stimulation is required for the nuclear retention of Id2 by preventing its nuclear export via CRM1/exportin.

Nuclear retention of Id2 requires Ser-5 phosphorylation by RANK signaling in the lactating mammary gland. In order to investigate whether the nuclear retention of Id2 requires Ser-5 phosphorylation by RANK signaling in developing mammary glands, we generated MMTV-*HA-Id2* and MMTV-*HA-Id2*^{S5A} transgenic (*Id2*Tg and *Id2*^{S5A}Tg, respectively) mice (Fig. 2A to D). Immunohistochemical staining with an anti-HA antibody showed that ectopic Id2 is abundantly expressed in the nuclei of MECs from *Id2*Tg mice on day 1 of lactation (L1) (Fig. 2G and H), while it was exclusively localized in the cytoplasm of MECs from the nonpregnant mice (Fig. 2E and F), indicating that nuclear localization of Id2 is regulated by a pregnancy/lactation-related hormone or factor. Because RANKL expression progressively increases during pregnancy and reaches high levels during lactation (10), we examined whether nuclear retention of Id2 requires RANK signaling. Indeed, in the *Id2*Tg; *RANKL*$^{-/-}$ mice at L1, exogenous Id2 was localized exclusively in the cytoplasm (Fig. 2I and J), indicating that nuclear localization of Id2 requires the activation of RANK signaling.

To further examine whether the nuclear localization of Id2 in the lactating mammary gland is dependent on Ser-5 phosphorylation of Id2, we performed immunohistochemical analysis using L1 *Id2*^{S5A}Tg mammary tissues. Mutant Id2^{S5A} that could not be phosphorylated by RANKL stimulation was exclusively localized in the cytoplasm of MECs from L1 *Id2*^{S5A}Tg mice, while endogenous Id2 was localized in the nuclei of MECs from the same mice (Fig. 2K to N). Consistently, Ser-5 phosphorylation was detected in the L1 *Id2*Tg mammary tissues, but not in the mammary tissues from virgin mice (Fig. 2O). In addition, Ser-5 phosphorylation was not detected in the L1 *Id2*Tg; *RANKL*$^{-/-}$ mammary tissues, indicating that it requires RANK signaling (Fig. 2P). Taken together, our results demonstrate that nuclear retention of Id2 requires Ser-5 phosphorylation via RANK signaling.

Forced expression of Id2 completely rescues defective mammary gland development of Id2-deficient mice. In order to test whether ectopically expressed Id2 in *Id2*Tg mice functions the same as the wild-type protein in mammary gland development, we crossed *Id2*$^{-/-}$ mice with one of the *Id2*Tg lines (line 86). Previous studies have reported that the mammary glands of *Id2*$^{-/-}$ mice are defective because of incorrect development of the lobuloalveolar structure, resulting in the death of newborns (28, 30). As expected, newborns of *Id2*Tg; *Id2*$^{-/-}$ mothers thrived well until adulthood. In addition, whole-mount carmine-alum staining and histological analyses of L1 mammary tissues showed that the developmental defect of the mammary gland in the *Id2*$^{-/-}$ mice was completely rescued by the ectopic expression of Id2 in *Id2*Tg; *Id2*$^{-/-}$ mice ($n = 9$) (Fig. 3A to F).

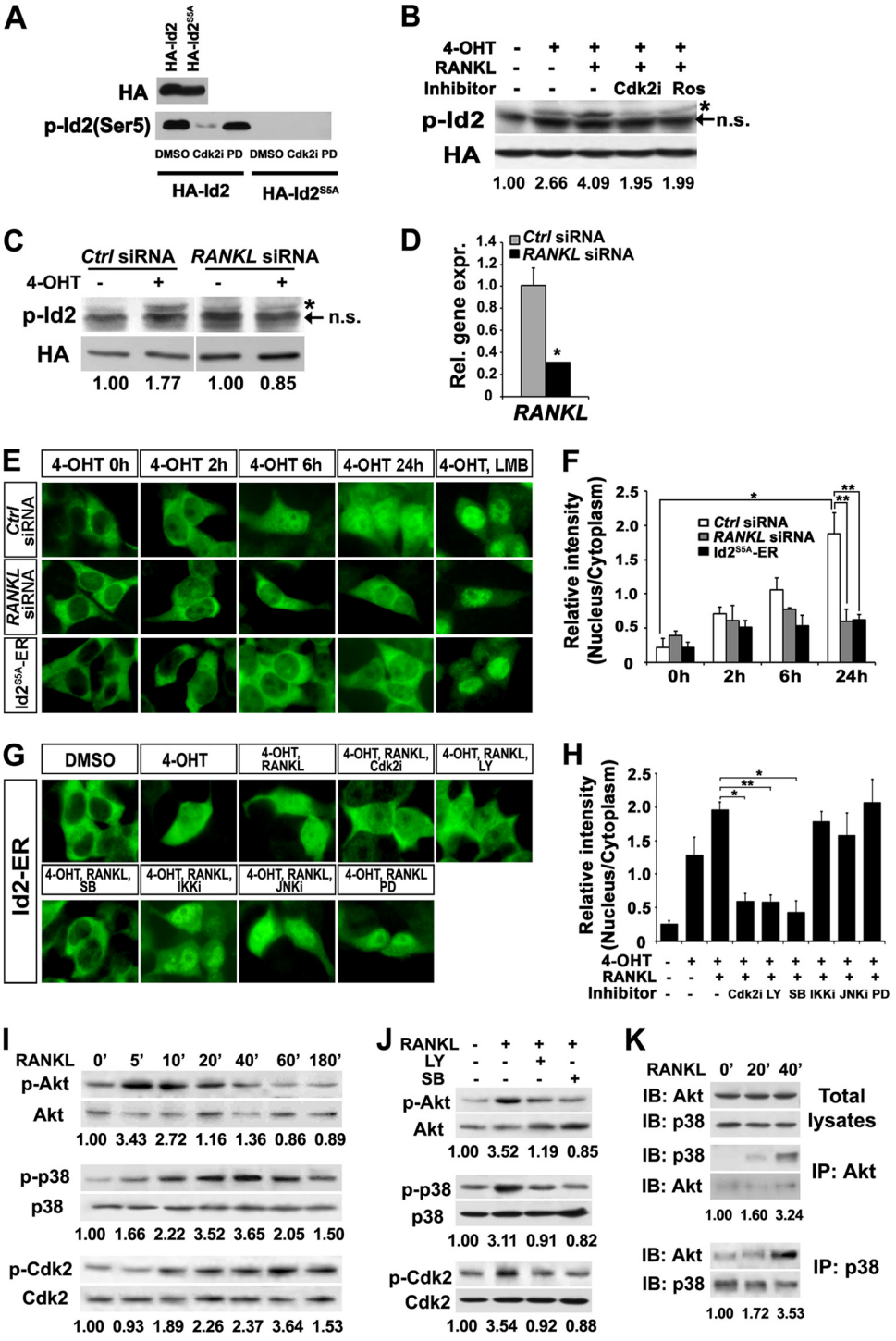

FIG. 1. Inhibition of CRM1/exportin-dependent nuclear export of Id2 by RANKL stimulation. (A) Western blot analysis of HA and p-Id2 (Ser-5) in lysates from HA-Id2- and HA-Id2^{S5A}-expressing MCF7 cell lines. Cdk2 inhibitor (Cdk2i) and Erk inhibitor (PD) were pretreated for 3 h before cell harvest. (B and C) MCF7 cells stably expressing HA-Id2-ER (Id2-ER MCF7 cells) were cultured in the presence (+) or absence (−) of 4-OHT, RANKL, Cdk2i, and roscovitine (Ros) (B), and Id2-ER MCF7 cells transfected with control or *RANKL* siRNA were cultured in the presence or absence of 4-OHT (C). Western blots were performed with anti-HA and anti-p-Id2 (Ser-5) antibodies. HA was used as a loading control. The arrows indicate nonspecific (n.s.) bands, and the asterisks represent p-Id2 (Ser-5) bands. The numbers at the bottom indicate the relative intensities of the bands. (D) Real-time RT-PCR analysis of the *RANKL* gene showed the efficiency of *RANKL* siRNA in the Id2-ER MCF7 cells. Significant difference: *, $P = 0.0005$. Rel. gene expr., relative gene expression. The error bars indicate standard deviations (SD). (E) Id2-ER MCF7 cells (top and middle rows) or HA-Id2^{S5A}-ER cells (bottom row) were cultured in the presence of 4-OHT for the indicated times. LMB was added for 3 h after 4-OHT treatment. Fixed cells were stained with an anti-HA antibody (green). (F) The relative intensity (nucleus/cytoplasm) of the fluorescence in panel E was quantified using Image-Pro Plus software. Over 80 cells were analyzed in each case. Significant differences: *, $P < 0.0001$, and **, $P = 0.03$. (G) Id2-ER-MCF7 cells were cultured in the presence or absence of 4-OHT, RANKL, and kinase inhibitors. Six

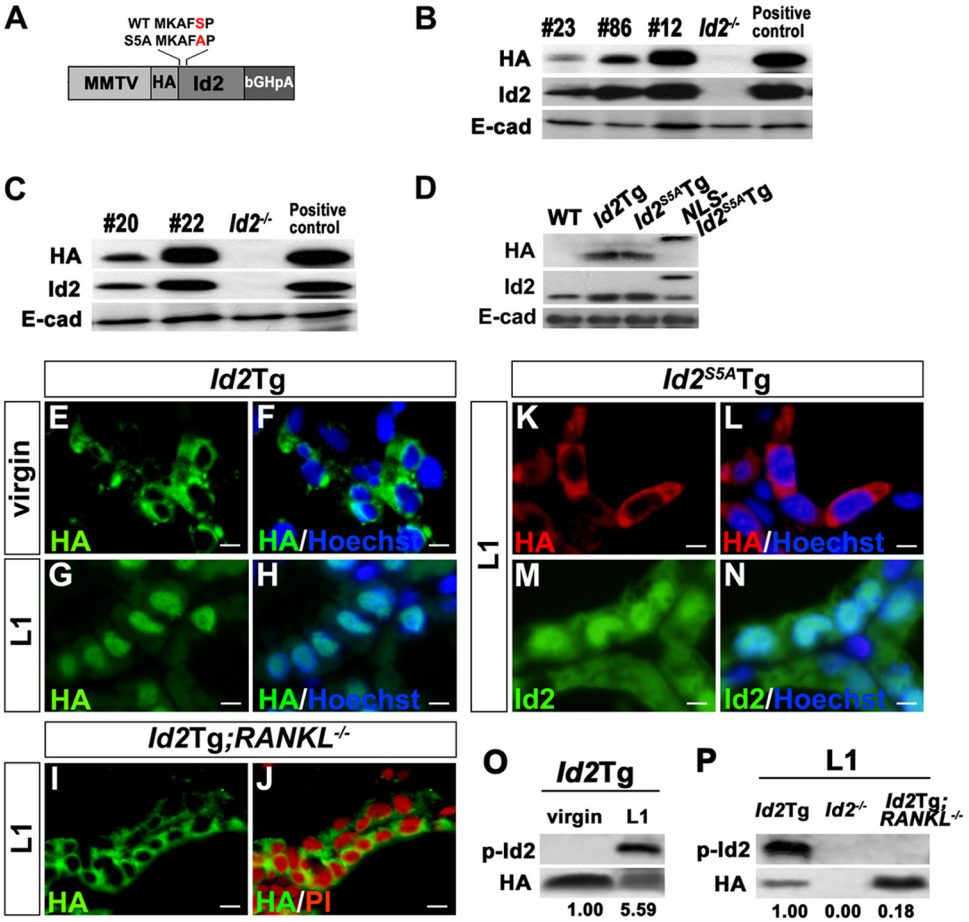

FIG. 2. Ser-5 phosphorylation-dependent nuclear retention of Id2 by RANK signaling. (A) Schematic representations of the MMTV-*Id2* (*Id2*Tg) and -$Id2^{S5A}$ ($Id2^{S5A}$Tg) transgenic constructs. bGHpA, bovine growth hormone polyadenylation signal. (B to D) Western blot analysis of HA and Id2 in tissue lysates from *Id2*Tg lines 23, 86, and 12 (B), $Id2^{S5A}$Tg lines 20 and 22 (C), and *Id2*Tg (line 86), $Id2^{S5A}$Tg (line 20), and *NLS-*$Id2^{S5A}$Tg (D) mammary glands at L1. E-cadherin (E-cad) was used as a loading control. Cell lysates from MCF7 cells expressing HA-Id2 were used as a positive control. Tissue lysates from $Id2^{-/-}$ mammary glands were used as a negative control. (E to N) Tissue sections of the mammary glands from virgin *Id2*Tg (E and F), L1 *Id2*Tg (G and H), L1 *Id2*Tg; $RANKL^{-/-}$ (I and J), and L1 $Id2^{S5A}$Tg (K to N) mice were stained with anti-HA and anti-Id2 antibodies. Nuclear DNA was stained with Hoechst (blue) or propidium iodide (PI) (red). Scale bars, 5 μm. The data were analyzed in alveolar structures. The images in panels I to L were taken using a confocal microscope. (O and P) Western blots were performed on the lysates of mammary tissues from *Id2*Tg mice (virgin) and at L1 (O) and from *Id2*Tg and *Id2*Tg; $RANKL^{-/-}$ mice at L1 (P). HA was used as a loading control. The lysate from $Id2^{-/-}$ mammary tissue was used as a negative control. The numbers at the bottom indicate the relative intensities of the bands.

Furthermore, immunohistochemical analysis showed that the Id2 protein in the *Id2*Tg; $Id2^{-/-}$ mice is expressed in the nuclei of MECs (Fig. 3I), as occurs in wild-type (WT) mice (Fig. 3G).

We performed terminal deoxynucleotidyltransferase-mediated dUTP-biotin nick end labeling (TUNEL) (Fig. 3J to L) and BrdU incorporation assays (Fig. 3M to O) in the L1 mammary epithelia from WT (Fig. 3J and M), $Id2^{-/-}$ (Fig. 3K and N), and *Id2*Tg; $Id2^{-/-}$ (Fig. 3L and O) mice. As expected, we found that the increased apoptosis and abnormal proliferation in $Id2^{-/-}$ MECs were rescued by the ectopic expression of Id2. The apoptotic index (Fig. 3S) and cellular proliferation (Fig. 3T) of the epithelia of *Id2*Tg; $Id2^{-/-}$ mice were similar to those of WT mice, showing that the ectopic expression of Id2 com-

hours after 4-OHT treatment, the cells were treated with kinase inhibitors for 3 h, and then the cells were stimulated with RANKL for 3 h prior to fixation. The fixed cells were stained with an anti-HA antibody (green). (H) The relative intensity (nucleus/cytoplasm) of the fluorescence was quantified using Image-Pro Plus software. Over 80 cells were analyzed in each case. Significant differences: *, $P < 0.0001$; **, $P = 0.0006$. (I) *RANKL* siRNA-treated MCF7 cells were stimulated with RANKL for the indicated times (minutes), and Western blot analyses were performed. (J) *RANKL* siRNA-treated MCF7 cells pretreated for 3 h with PI3K inhibitor (LY) and p38 MAPK inhibitor (SB) were stimulated with RANKL for 20 min (for p-Akt) and 40 min (for p-p38). (K) *RANKL* siRNA-treated MCF7 cells were stimulated with RANKL for the indicated times, and the cell lysates were immunoprecipitated with anti-Akt and anti-p38 antibodies. IB, immunoblot. (I to K) The numbers at the bottom indicate the relative intensities of the bands. A representative of three independent experiments is shown.

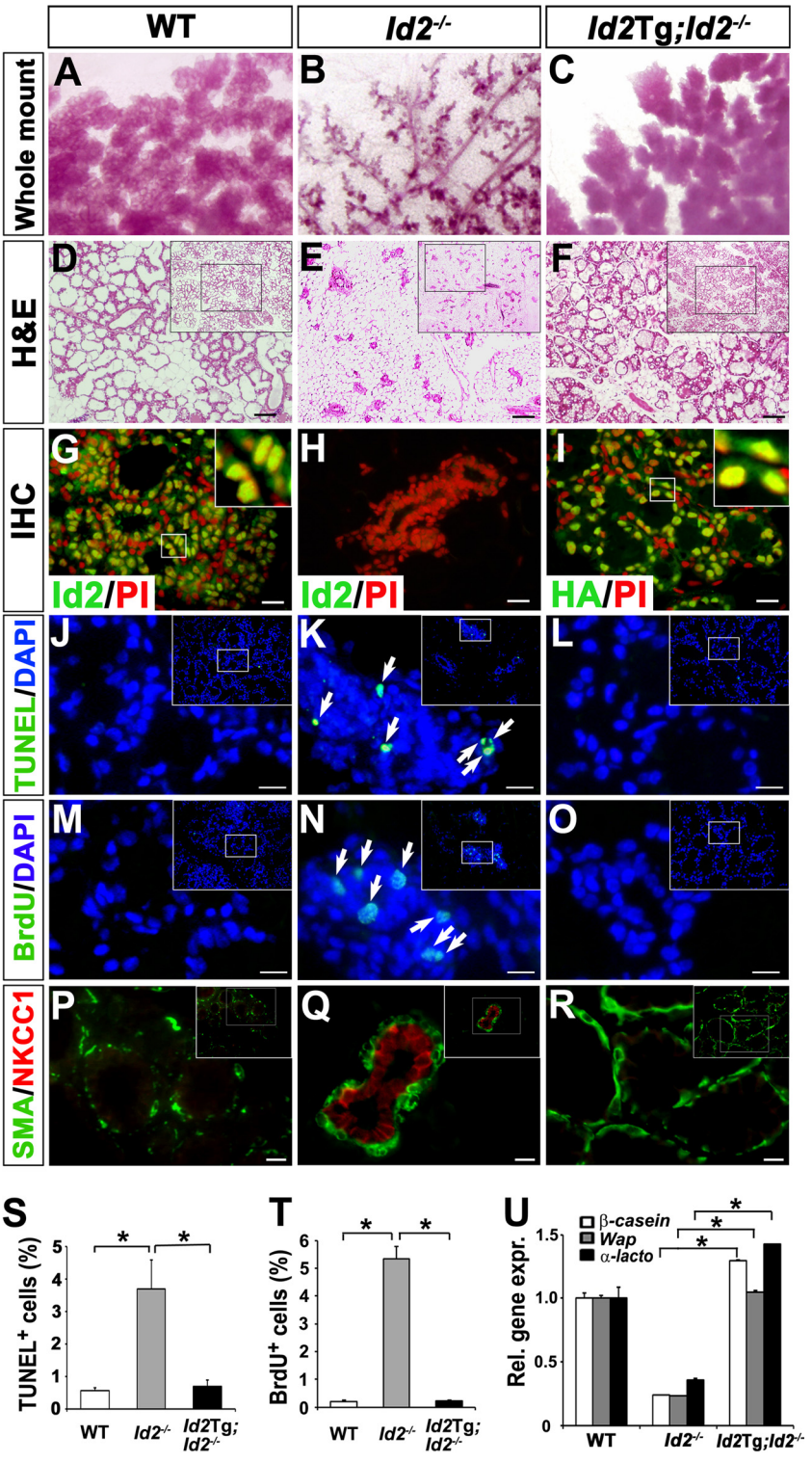

FIG. 3. Forced expression of Id2 in $Id2^{-/-}$ mammary epithelia. (A to F) Whole-mount carmine-alum staining (A to C) and H&E staining (D to F) of mammary glands from WT (A and D), $Id2^{-/-}$ (B and E), and *Id2*Tg; $Id2^{-/-}$ (C and F) mice at L1. The insets (D to F) show images at lower magnification. Scale bars, 100 μm. (G to I) Tissue sections of the mammary glands from WT (G), $Id2^{-/-}$ (H), and *Id2*Tg; $Id2^{-/-}$ (I) mice at L1 were stained with anti-Id2 (G and H) and anti-HA (I) antibodies (green). Nuclear DNA was stained with PI (red). Higher-magnification images (insets) show nuclear localization of Id2 in WT (G) and *Id2*Tg; $Id2^{-/-}$ (I) mammary glands. Scale bars, 20 μm. IHC, immunohistochemistry. (J to O, S, and T) TUNEL (J to L; green) and BrdU (M to O; green) staining of L1 WT (J and M), $Id2^{-/-}$ (K and N), and *Id2*Tg; $Id2^{-/-}$ (L and O) mammary tissues. Mice were injected with BrdU 3 h before analysis. The arrows indicate TUNEL-positive cells (K) and BrdU-positive cells (N). Nuclear DNA was stained with DAPI (4′,6-diamidino-2-phenylindole) (blue). Scale bars, 12 μm. The numbers of TUNEL-positive cells (S) and BrdU-positive cells (T) per 10^5 μm^2 were determined. The data are shown as means and SD. Significant differences: *, $P = 0.0002$ (S) and

pletely rescues the survival and abnormal proliferation in the *Id2*$^{-/-}$ MECs.

We next examined the differentiation status of the *Id2*Tg; *Id2*$^{-/-}$ mammary epithelia using antibodies against SMA, a marker of myoepithelial cells, and NKCC1, a Na-K-Cl cotransporter that is expressed at high levels in ductal epithelial cells from virgin mice but not in lactating secretory alveolar cells (29, 37). In the *Id2*Tg; *Id2*$^{-/-}$ mammary epithelium at L1, NKCC1 was undetectable (Fig. 3R), as in WT epithelia (Fig. 3P), while it was still detected in *Id2*$^{-/-}$ epithelia (Fig. 3Q). We also carried out quantitative real-time RT-PCR analysis to examine the expression of milk genes (β-*casein*, *whey acidic protein* [*Wap*], and α-*lactoalbumin*) in the *Id2*Tg; *Id2*$^{-/-}$ mammary epithelium at L1. As expected, the expression of the milk genes was completely rescued in *Id2*Tg; *Id2*$^{-/-}$ mammary epithelia (Fig. 3U). Taken together, these results show that the mammary defects of *Id2*$^{-/-}$ mice were completely rescued by ectopic expression of Id2 in *Id2*Tg; *Id2*$^{-/-}$ mice.

Inability of ectopic Id2 to rescue defective mammary gland development in RANKL-deficient mice. We investigated whether ectopic expression of Id2 in the mammary tissues is able to rescue defective mammary gland development in *RANKL*$^{-/-}$ mice. A previous study reported that pups nursed by *RANKL*$^{-/-}$ mothers died within 48 h of birth because of failure of maternal milk production (10). As expected, pups nursed by *Id2*Tg; *RANKL*$^{-/-}$ mothers also died within 48 h of birth and did not have milk in their stomachs (data not shown). To examine the mammary gland development of *Id2*Tg; *RANKL*$^{-/-}$ mice, we performed whole-mount carmine-alum staining (Fig. 4A to C) and hematoxylin and eosin (H&E) staining (Fig. 4D to F) of mammary glands from the crossed mice at L1. *Id2*Tg; *RANKL*$^{-/-}$ mice showed failure in the development of the lobuloalveolar structure (Fig. 4C and F), as observed in *RANKL*$^{-/-}$ mice (Fig. 4B and E).

To examine whether the increased apoptosis and abnormal proliferation of MECs in *RANKL*$^{-/-}$ mice could be rescued by the ectopic expression of Id2, we performed a TUNEL assay (Fig. 4G to I) and a BrdU incorporation assay (Fig. 4J to L). The apoptotic index (Fig. 4P) and cellular proliferation (Fig. 4Q) of the epithelia of *Id2*Tg; *RANKL*$^{-/-}$ mice ($n = 6$) were similar to those of *RANKL*$^{-/-}$ mice ($n = 8$), indicating that the ectopic expression of Id2 alone cannot rescue the increased apoptosis and abnormal proliferation in the absence of RANK signaling. We next examined the differentiation status of the *Id2*Tg; *RANKL*$^{-/-}$ mammary epithelia using antibodies against SMA and NKCC1. In the WT mammary epithelium at L1, NKCC1 was undetected (Fig. 4M), while it was detected in *RANKL*$^{-/-}$ ($n = 8$) (Fig. 4N) and *Id2*Tg; *RANKL*$^{-/-}$ ($n = 6$) (Fig. 4O) epithelia. Moreover, quantitative real-time RT-PCR analysis revealed that *Id2*Tg;*RANKL*$^{-/-}$ mice ($n = 6$) also had defective expression of the milk genes, β-*casein*, *Wap*, and α-*lactoalbumin* (Fig. 4R). Taken together, these results show that forced expression of cytoplasmic Id2 is not sufficient to rescue the defects in mammary gland development of *RANKL*$^{-/-}$ mice.

Forced expression of NLS-Id2^{S5A} completely rescues defective mammary gland development of Id2-deficient mice. In order to investigate the physiological relevance of nuclear-located Id2 as signaling downstream of RANK in developing mammary glands, we generated MMTV-*HA-NLS-Id2*^{S5A} transgenic (*NLS-Id2*^{S5A}Tg) mice (Fig. 5A and B). To examine whether the NLS-Id2^{S5A} protein in *NLS-Id2*^{S5A}Tg mice functions properly, we bred *Id2*$^{-/-}$ mice with *NLS-Id2*^{S5A}Tg mice. Whole-mount carmine-alum (Fig. 5C to E) and H&E (Fig. 5F to H) staining of L1 mammary tissues revealed that the developmental defects of the mammary gland in *Id2*$^{-/-}$ mice (Fig. 5D and G) were completely rescued by the ectopic expression of NLS-Id2^{S5A} in *NLS-Id2*^{S5A}Tg; *Id2*$^{-/-}$ mice ($n = 4$) (Fig. 5E and H). Immunohistochemical staining with an anti-HA antibody revealed that the NLS-Id2^{S5A} protein was expressed exclusively in the nucleus (Fig. 5K). In addition, quantitative real-time RT-PCR analysis showed that expression of the milk genes, β-*casein*, *Wap*, and α-*lactoalbumin*, was significantly increased in *NLS-Id2*^{S5A}Tg; *Id2*$^{-/-}$ mammary epithelia compared to *Id2*$^{-/-}$ mammary epithelia (Fig. 5L). Thus, we conclude that the transgenic NLS-Id2^{S5A} protein is expressed in the nuclei of MECs and functions properly, even though Ser-5 is not phosphorylated by RANK signaling. These results suggest that nuclear retention, rather than phosphorylation of Ser-5 of Id2, is required for mammary gland development.

Forced expression of NLS-Id2^{S5A} significantly rescues defective mammary gland development in *RANKL*$^{-/-}$ mice. So far, we had shown that RANK signaling induces the nuclear retention of Id2 by Cdk2-dependent phosphorylation of Ser-5 of Id2 and determined that nuclear retention of Id2 is critically important for mammary gland development during pregnancy. We next investigated whether enforced expression of NLS-tagged-Id2^{S5A} protein could rescue defective mammary gland development in *RANKL*$^{-/-}$ mice.

When we bred *NLS-Id2*^{S5A}Tg mice with *RANKL*$^{-/-}$ mice, pups nursed by *NLS-Id2*^{S5A}Tg; *RANKL*$^{-/-}$ mothers ($n = 3$) surprisingly lived for 4 days (they died after 4 days), while pups nursed by *RANKL*$^{-/-}$ mothers ($n = 12$) died within 48 h of birth (10). Moreover, 1-day-old pups nursed by *RANKL*$^{-/-}$ mothers lacked milk in their stomachs (Fig. 6A); however, pups nursed by *NLS-Id2*^{S5A}Tg; *RANKL*$^{-/-}$ mothers had milk in their stomachs for 3 days (Fig. 6B). Intriguingly, whole-mount carmine-alum and H&E staining of mammary glands on day 14.5 of pregnancy (P14.5) (Fig. 6C to H) and L1 (Fig. 6I to N) revealed that the developmental defect in *RANKL*$^{-/-}$ mice (P14.5, $n = 5$; L1, $n = 9$) (Fig. 6D, G, J, and M) was rescued to a large extent by the ectopic expression of NLS-

$P < 0.0001$ (T). (P to R) Tissue sections of mammary glands from WT (P), *Id2*$^{-/-}$ (Q), and *Id2*Tg; *Id2*$^{-/-}$ (R) mice at L1 were stained with anti-SMA (green) and anti-NKCC1 (red) antibodies. Note that the luminal epithelial cells from WT (P) and *Id2*Tg; *Id2*$^{-/-}$ (R) mice have no expression of NKCC1, while those from *Id2*$^{-/-}$ (Q) mice show NKCC1 expression. The insets (P to R) show lower-magnification images. Scale bars, 10 μm. (U) Real-time RT-PCR analysis of milk genes (β-*casein*, *Wap*, and α-*lactoalbumin*) from WT, *Id2*$^{-/-}$, and *Id2*Tg; *Id2*$^{-/-}$ mammary tissues at L1. *CK18* was used for data normalization. The data are shown as means and SD. A representative of three independent experiments is shown. Significant differences: *, $P < 0.0001$.

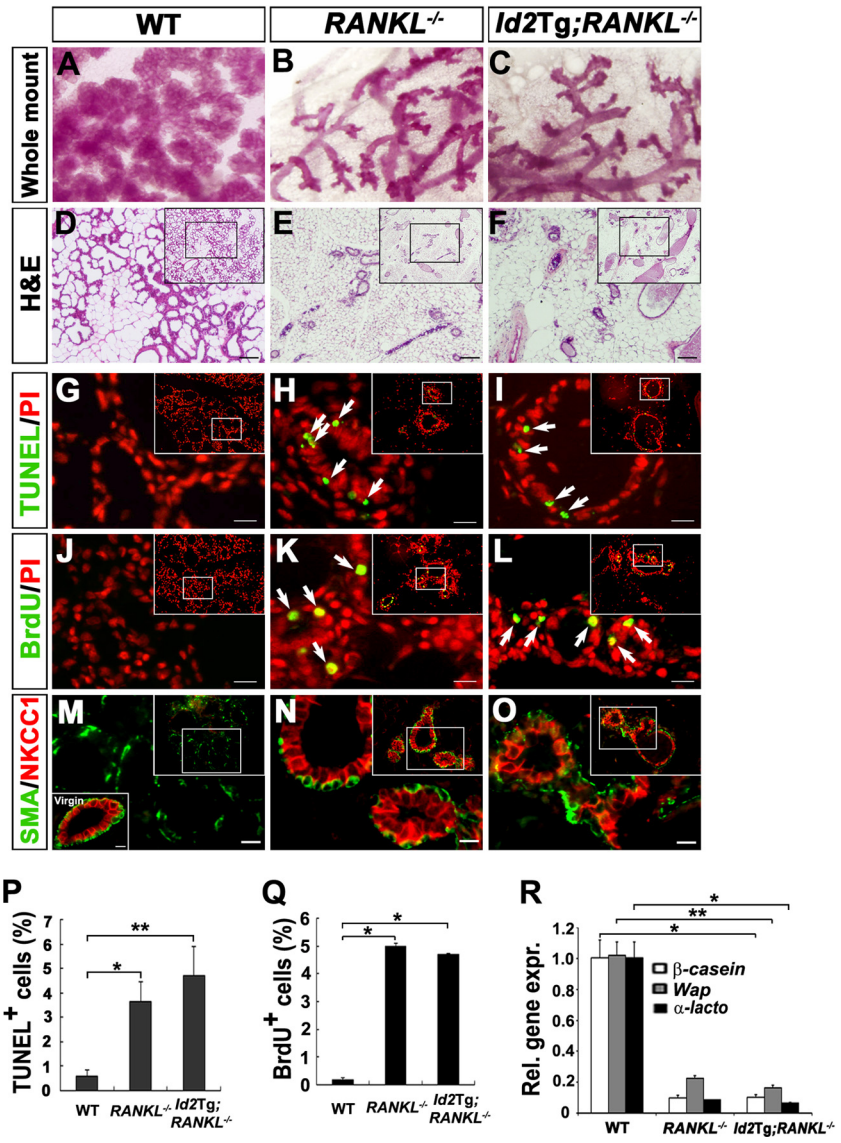

FIG. 4. Forced expression of Id2 in *RANKL*$^{-/-}$ mammary epithelia. (A to F) Whole-mount carmine-alum staining (A to C) and H&E staining (D to F) of mammary glands from WT (A and D), *RANKL*$^{-/-}$ (B and E), and *Id2*Tg; *RANKL*$^{-/-}$ (C and F) mice at L1. Scale bars, 100 μm. (G to L, P, and Q) TUNEL (G to I; green) and BrdU (J to L; green) staining of L1 WT (G and J), *RANKL*$^{-/-}$ (H and K), and *Id2*Tg; *RANKL*$^{-/-}$ (I and L) mammary tissues. Mice were injected with BrdU 3 h before analysis. The arrows indicate TUNEL-positive cells (H and I) and BrdU-positive cells (K and L). Nuclear DNA was stained with PI (red). Scale bars, 12 μm. The numbers of TUNEL-positive cells (P) and BrdU-positive cells (Q) per 10^5 μm^2 were determined. The data are shown as means and SD. Significant differences: *, $P = 0.0004$ (P); **, $P = 0.001$ (P); and *, $P < 0.0001$ (Q). (M to O) Tissue sections of mammary glands from WT (M), *RANKL*$^{-/-}$ (N), and *Id2*Tg; *RANKL*$^{-/-}$ (O) mice at L1 were stained with anti-SMA (green) and anti-NKCC1 (red) antibodies. Note that the luminal epithelial cells from WT mice (M) have no expression of NKCC1, while those from *RANKL*$^{-/-}$ (N) and *Id2*Tg; *RANKL*$^{-/-}$ (O) mice show NKCC1 expression. The insets show lower-magnification images. The left bottom inset in panel M shows virgin tissue stained with anti-SMA (green) and anti-NKCC1 (red) antibodies as a control. Scale bars, 10 μm. (G to Q) The data were analyzed in alveolar structures. (R) Real-time RT-PCR analysis of milk genes (β-*casein*, *Wap*, and α-*lactoalbumin*) from WT, *RANKL*$^{-/-}$, and *Id2*Tg; *RANKL*$^{-/-}$ mammary tissues at L1. *CK18* was used for data normalization. The data are shown as means and SD. Significant differences: *, $P < 0.0002$, and **, $P < 0.004$. A representative of three independent experiments is shown.

Id2^{S5A} in *NLS-Id2*^{S5A}Tg; *RANKL*$^{-/-}$ mice (P14.5, $n = 4$; L1, $n = 4$) (Fig. 6E, H, K, and N). In WT females, pregnancy hormones induce the proliferation of ductal epithelium and sprouting of alveolar buds during midpregnancy (Fig. 6C and F). Subsequently, lactogenic differentiation of the alveolar buds occurs, resulting in the formation of fully developed lobuloalveolar structures and primary ducts at L1 (10, 30) (Fig. 6I and L). As reported previously (10), differentiation and expansion of the alveolar buds into mature lobuloalveolar mammary structures was completely arrested in *RANKL*$^{-/-}$ females (Fig. 6D, G, J, and M). However, *NLS-Id2*^{S5A}Tg; *RANKL*$^{-/-}$ females showed enlarged multilobed ductal structures, which are abnormally premature alveolar ducts (Fig. 6E and H), unlike the sprouted alveolar buds in the P14.5 WT mammary tissues (Fig. 6K and N). These enlarged ductal structures were differentiated into alveolar-like, milk-producing ducts instead of the

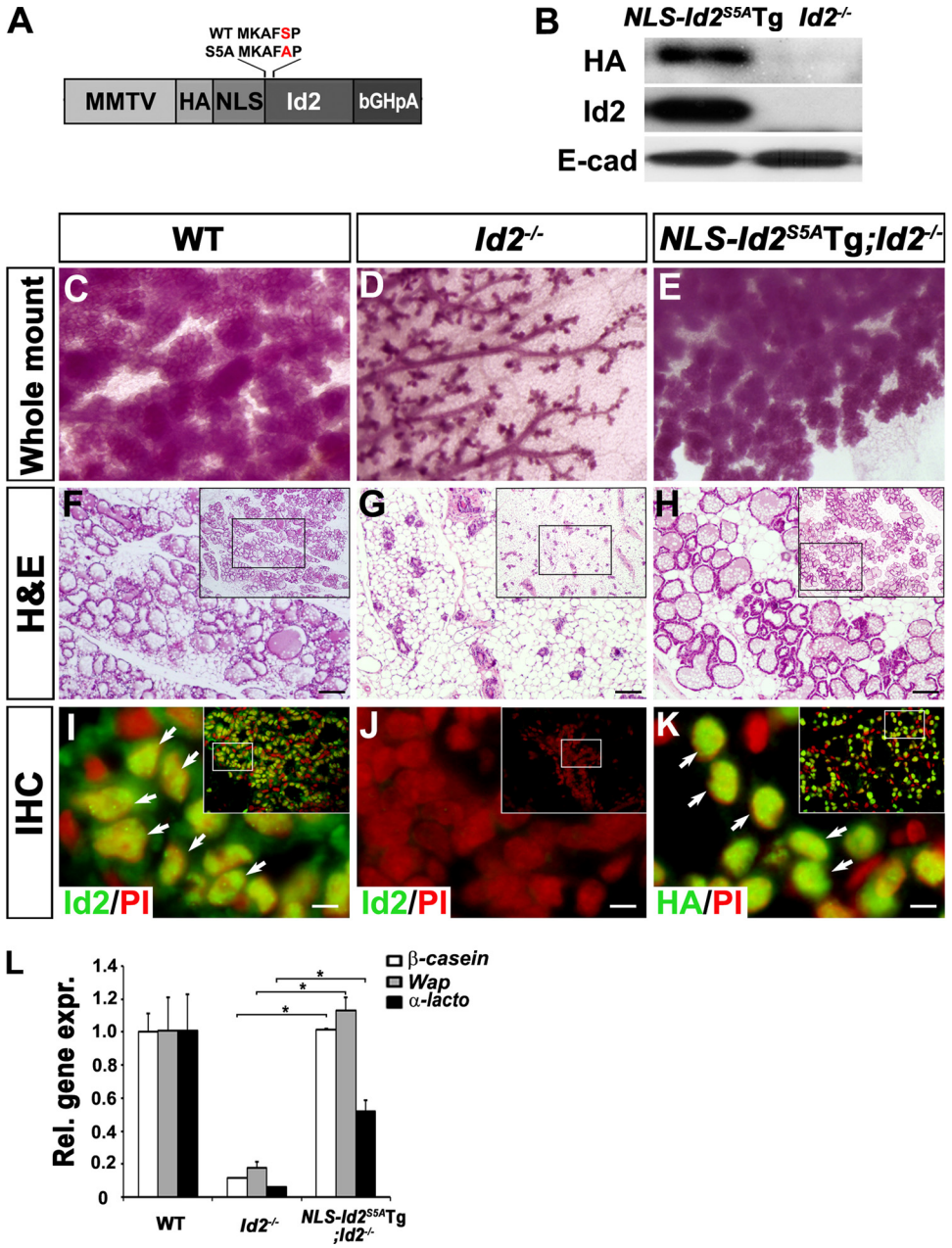

FIG. 5. Forced expression of NLS-Id2^{S5A} in *Id2*$^{-/-}$ mammary glands. (A) Schematic representation of the MMTV-*NLS-Id2*^{S5A} (*NLS-Id2*^{S5A}Tg) transgenic construct. (B) Western blot analysis of HA and Id2 in tissue lysates from *NLS-Id2*^{S5A}Tg mammary glands at L1. E-cadherin was used as a loading control. Tissue lysates from *Id2*$^{-/-}$ mammary glands were used as a negative control. (C to H) Whole-mount carmine-alum staining (C to E) and H&E staining (F to H) of mammary glands from WT (C and F), *Id2*$^{-/-}$ (D and G), and *NLS-Id2*^{S5A}Tg; *Id2*$^{-/-}$ (E and H) mice at L1. The insets show lower-magnification images. Scale bars, 100 μm. (I to K) Tissue sections of the mammary glands from WT (I), *Id2*$^{-/-}$ (J), and *NLS-Id2*^{S5A}Tg; *Id2*$^{-/-}$ (K) mice at L1 were stained with anti-Id2 (I and J) and anti-HA (K) antibodies (green). Nuclear DNA was stained with PI (red). The arrows indicate nuclear-localized Id2 in L1 tissues from WT (I) and *NLS-Id2*^{S5A}Tg; *Id2*$^{-/-}$ (K) mice. The insets are lower-magnification images. Scale bars, 5 μm. (L) Real-time RT-PCR analysis of milk genes (β-*casein*, *Wap*, and α-*lactoalbumin*) from WT, *Id2*$^{-/-}$, and *NLS-Id2*^{S5A}Tg; *Id2*$^{-/-}$ mammary tissues at L1. *CK18* was used for data normalization. The data are shown as means and SD. Significant differences: *, $P < 0.0001$. A representative of three independent experiments is shown.

lobuloalveolar structures observed in WT mammary tissues (Fig. 6K and N), suggesting that impaired sprouting of alveolar buds in the *NLS-Id2*^{S5A}Tg; *RANKL*$^{-/-}$ mammary epithelia might be due to their premature differentiation in the absence of appropriate proliferation during pregnancy. Taken together, these results show that the defective mammary gland development of the *RANKL*$^{-/-}$ mice is substantially rescued by the nuclear retention of Id2^{S5A} in *NLS-Id2*^{S5A}Tg; *RANKL*$^{-/-}$ mice.

RANK-Id2 signaling plays essential roles in the survival and lactogenic differentiation, but not proliferation, of mammary epithelial cells. RANK signaling has been implicated in

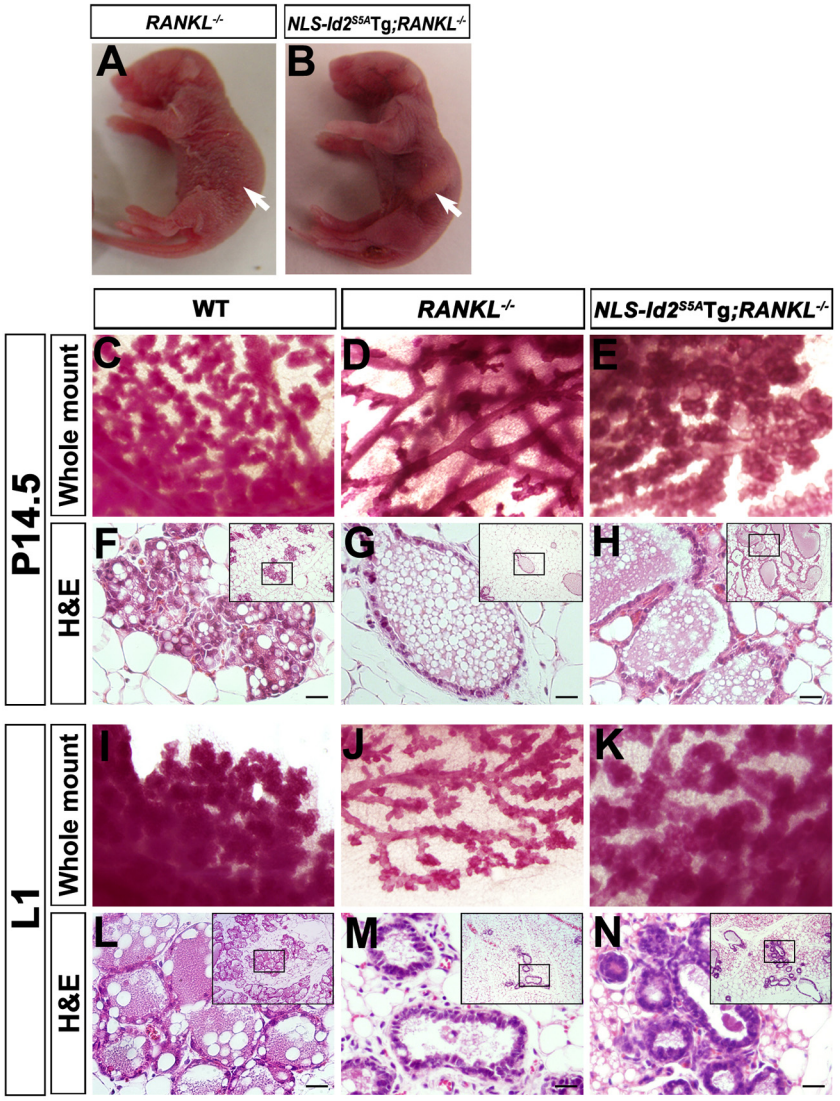

FIG. 6. Rescue of *RANKL*$^{-/-}$ mammary glands by forced expression of NLS-Id2^{S5A}. (A and B) Photographs of pups from *RANKL*$^{-/-}$ (A) and *NLS-Id2*^{S5A}Tg; *RANKL*$^{-/-}$ (B) mothers. Note that the pup from *NLS-Id2*^{S5A}Tg; *RANKL*$^{-/-}$ mice (B) has milk in its stomach, in contrast to the pup from *RANKL*$^{-/-}$ mice (A) (arrows). (C to N) Whole-mount carmine-alum staining (C to E and I to K) and H&E staining (F to H and L to N) of mammary glands from WT (C, F, I, and L), *RANKL*$^{-/-}$ (D, G, J, and M), and *NLS-Id2*^{S5A}Tg; *RANKL*$^{-/-}$ (E, H, K, and N) mice at P14.5 (C to H) and L1 (I to N). The insets are lower-magnification images. Scale bars, 20 μm.

multiple events, including the proliferation, survival, and lactogenic differentiation of MECs during pregnancy (10). Substantial, albeit partial, rescue of the mammary gland defect in *NLS-Id2*^{S5A}Tg; *RANKL*$^{-/-}$ mice suggests that nuclear expression of Id2^{S5A} might affect a certain cellular event(s) during mammary gland development conducted by RANK signaling. To determine what defect(s) of *RANKL*$^{-/-}$ mice is rescued by the forced expression of nuclear Id2^{S5A}, we first performed a TUNEL assay with the L1 mammary epithelia (Fig. 7D to F). The apoptotic index of the epithelia of *NLS-Id2*^{S5A}Tg; *RANKL*$^{-/-}$ mice (0.85%) (n = 4) was markedly lower than that of *RANKL*$^{-/-}$ mice (4.37%) (n = 9) (Fig. 7K). Similar results were also observed in the P14.5 mammary epithelia (Fig. 7A to C and J). Moreover, immunohistochemical staining (Fig. 7G to I) with an anti-active-caspase 3 antibody also showed that increased apoptosis in *RANKL*$^{-/-}$ mice (Fig. 7H) was completely rescued by the presence of nuclear Id2^{S5A} in *NLS-Id2*^{S5A}; *RANKL*$^{-/-}$ mice (Fig. 7I). Consistently, quantitative real-time RT-PCR analysis showed that the expression of antiapoptotic genes, *Bcl-2* and *Bcl-X*$_L$, was significantly increased in *NLS-Id2*^{S5A}Tg; *RANKL*$^{-/-}$ mammary epithelia compared to *RANKL*$^{-/-}$ mammary epithelia (Fig. 7L). These results show that the nuclear retention of Id2 due to RANK signaling plays an essential role in the survival of MECs.

Because pups from *NLS-Id2*^{S5A}Tg; *RANKL*$^{-/-}$ mothers had milk in their stomachs (Fig. 6B), we examined the differentiation status of the mothers' mammary epithelia by immunohistochemical analysis. Interestingly, the expression of NKCC1 was not detected in tissues of P14.5 and L1 *NLS-Id2*^{S5A}Tg; *RANKL*$^{-/-}$ mice, as in WT mammary epithelia (Fig. 8A, C, D,

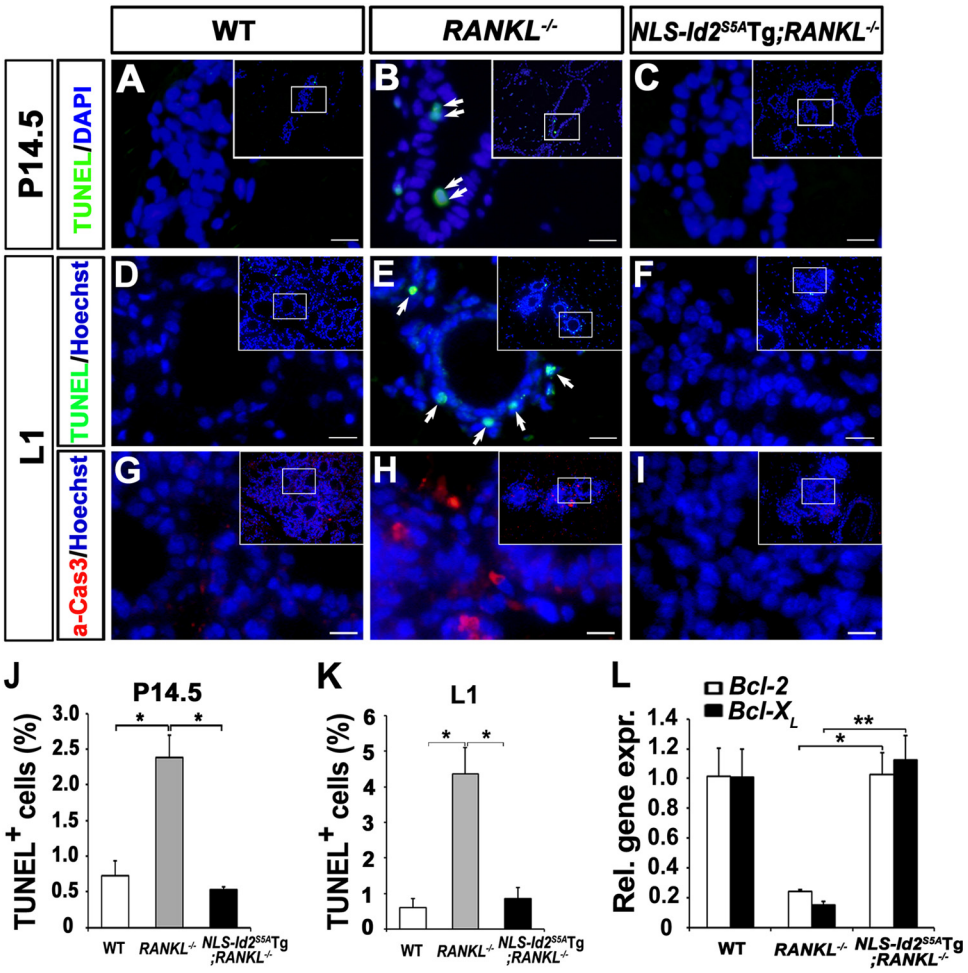

FIG. 7. Rescued survival in *NLS-Id2*^{S5A}Tg; *RANKL*$^{-/-}$ mice by forced expression of NLS-Id2^{S5A}. (A to F) TUNEL staining (green) in WT (A and D), *RANKL*$^{-/-}$ (B and E), and *NLS-Id2*^{S5A}Tg; *RANKL*$^{-/-}$ (C and F) mammary tissues at P14.5 (A to C) and L1 (D to F). The arrows in panels B and E indicate the TUNEL-positive cells. Nuclear DNA was stained with DAPI or Hoechst (blue).The insets are lower-magnification images. Scale bars, 12 μm. (G to I) Immunofluorescence staining for active caspase 3 (red) in L1 WT (G), *RANKL*$^{-/-}$ (H), and *NLS-Id2*^{S5A}Tg; *RANKL*$^{-/-}$ (I) mammary tissues. Nuclear DNA was stained with Hoechst (blue). The insets are lower-magnification images. Scale bars, 12 μm. (J and K) The number of TUNEL-positive cells per 10^5 μm^2 was determined from mammary tissue sections at P14.5 (J) and L1 (K). The data are shown as means and SD. Significant differences: *, $P = 0.005$ (J) and $P < 0.0001$ (K). (A to K) The data were analyzed in alveolar structures. (L) Real-time RT-PCR analysis of anti-apoptotic genes (*Bcl-2* and *Bcl-X*$_L$) from WT, *RANKL*$^{-/-}$, and *NLS-Id2*^{S5A}Tg; *RANKL*$^{-/-}$ mammary tissues at L1. *CK18* was used for data normalization. The data are shown as means and SD. A representative of three independent experiments is shown. Significant differences: *, $P = 0.002$, and **, $P = 0.001$.

and F), but NKCC1 expression was retained in P14.5 and L1 *RANKL*$^{-/-}$ epithelia (Fig. 8B and E), suggesting that the nuclear retention of Id2 is important for cellular differentiation of mammary epithelia. Consistently, quantitative real-time RT-PCR analysis showed that expression of the milk genes was significantly increased in *NLS-Id2*^{S5A}Tg; *RANKL*$^{-/-}$ mammary epithelia compared to *RANKL*$^{-/-}$ mammary epithelia (Fig. 8G and H).

To further examine whether the proliferative defect of *RANKL*$^{-/-}$ mice is rescued by the forced expression of nuclear Id2^{S5A}, we performed BrdU incorporation with the mammary epithelia at P7.5. The proliferative index of P7.5 epithelia of *NLS-Id2*^{S5A}Tg; *RANKL*$^{-/-}$ mice (2.89%) ($n = 3$) was not significantly increased compared to the *RANKL*$^{-/-}$ mice (1.59%) ($n = 4$) (Fig. 8I to L). These data demonstrate that the ectopic expression of NLS-Id2^{S5A} cannot overcome the proliferative defect of the *RANKL*$^{-/-}$ mammary gland.

Collectively, these data show that the RANK-Id2 signaling pathway is essential for cellular survival and lactogenic differentiation, but not proliferation, of MECs during pregnancy.

DISCUSSION

The RANKL-RANK signaling pathway has been implicated in multiple events, the proliferation, survival, and lactogenic differentiation of MECs during pregnancy (10). In the present study, we found that RANK signaling induces the nuclear retention of Id2 by PI3K-p38 MAPK-Cdk2-mediated phosphorylation of Ser-5 of Id2, and nuclear retention of Id2 was shown to be essential for mammary gland development during

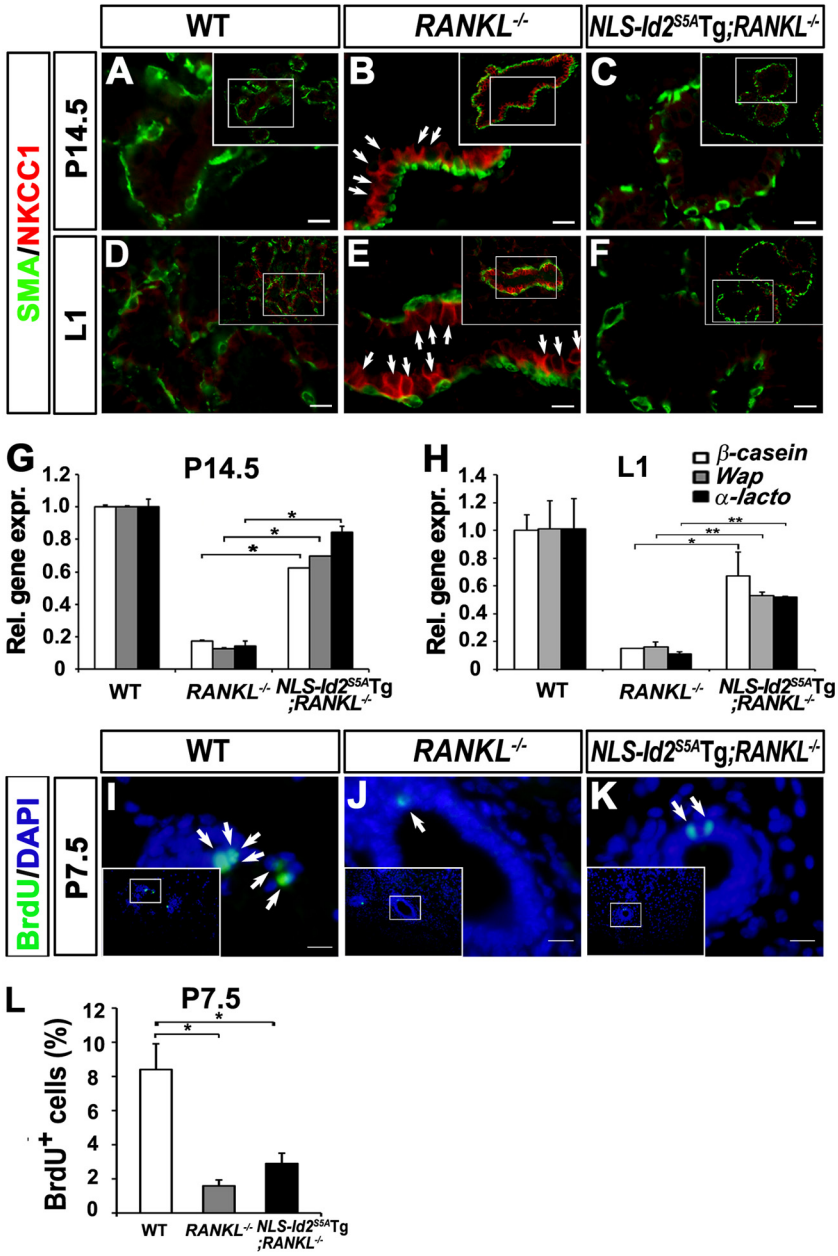

FIG. 8. Rescued lactogenic differentiation in *NLS-Id2*^{S5A}Tg; *RANKL*$^{-/-}$ mice by forced expression of NLS-Id2^{S5A}. (A to F) Immunofluorescence staining for SMA (green) and NKCC1 (red) in WT (A and D), *RANKL*$^{-/-}$ (B and E), and *NLS-Id2*^{S5A}Tg; *RANKL*$^{-/-}$ (C and F) mammary tissues at P14.5 (A to C) and L1 (D to F). Note that NKCC1-positive cells are present in the *RANKL*$^{-/-}$ mammary ducts (B and E) but absent from *NLS-Id2*^{S5A}Tg; *RANKL*$^{-/-}$ mammary ducts (C and F). The insets are lower-magnification images. Scale bars, 10 μm. (G and H) Real-time RT-PCR analysis of milk genes (β-*casein*, *Wap*, and α-*lactoalbumin*) from WT, *RANKL*$^{-/-}$, and *NLS-Id2*^{S5A}Tg; *RANKL*$^{-/-}$ mammary tissues at P14.5 (G) and L1 (H). *CK18* was used for data normalization. The data are shown as means and SD. A representative of three independent experiments is shown. Significant differences: *, $P < 0.0001$ (G) and $P = 0.002$ (H); **, $P = 0.001$ (H). (I to K) BrdU (green) staining of WT (I), *RANKL*$^{-/-}$ (J), and *NLS-Id2*^{S5A}Tg; *RANKL*$^{-/-}$ (K) mammary tissues at P7.5. Mice were injected with BrdU 3 h before analysis. The arrows indicate BrdU-positive cells. Nuclear DNA was stained with Hoechst (blue). The insets are lower-magnification images. Scale bars, 12 μm. (L) The number of BrdU-positive cells per 10^5 μm^2 was determined from the alveolar structure of P7.5 mammary tissue sections. The data are shown as means and SD. Significant difference: *, $P < 0.0001$. (A to F and I to L) The data were analyzed in alveolar structures.

pregnancy. Wild-type Id2, in the absence of RANK signaling in virgin mice, was expressed exclusively in the cytoplasm and failed to rescue the defective mammary gland development of *RANKL*$^{-/-}$ mice. In contrast, the forced nuclear expression of mutant Id2^{S5A} using a nuclear localization sequence rescued the increased apoptosis and defective differentiation of MECs observed in *RANKL*$^{-/-}$ mice, despite lack of phosphorylation of mutant Id2^{S5A} by RANK signaling. Furthermore, the forced nuclear expression of mutant Id2^{S5A} alone in virgin mice resulted in lactogenic differentiation, but not proliferation, of

MECs. Collectively, our data show that the RANK-Id2 signaling pathway plays a critical role in the survival and lactogenic differentiation of MECs during pregnancy.

RANK signaling-induced phosphorylation of Id2 inhibits its nuclear export. Id2 is regulated at multiple stages: transcription, degradation (24), and changes in its subcellular localization (21). Recent studies have shown that changes in the subcellular localization of the Id2 protein are implicated in diverse cellular contexts, including hematopoietic (41), neural (23, 35, 42), muscle (27), and renal (25) cells. However, how changes in localization lead to functional regulation by exogenous stimuli, such as growth factors, is unknown. It is likely that Id2 can pass freely through the nuclear pore by simple diffusion, but it is actively exported to the cytoplasm via CRM1/exportin (21). Since Id2 functions in the nucleus in diverse cellular contexts, it appears that exogenous stimuli lead to its nuclear localization. Indeed, we previously reported that RANK signaling induces nuclear translocation of Id2 (19). Moreover, RANK-induced Id2 nuclear translocation requires Cdk2 activity, implying that a phosphorylation event is involved. In this study, we found that Ser-5 of Id2 is readily phosphorylated by RANKL stimulation and that phosphorylation of this Ser-5 is required for the nuclear retention of Id2, as it prevents CRM1/exportin-mediated export of Id2 to the cytoplasm using MCF7 cells. In addition, by generating *Id2*Tg; *RANKL*$^{-/-}$ mice and *Id2*^{S5A}Tg mice, we directly demonstrated that RANK signaling is required for nuclear retention of Id2 by phosphorylating Ser-5 in lactating mammary glands.

Nuclear retention of Id2 is sufficient for survival and lactogenic differentiation of MECs. Since RANK signaling regulates multiple events—proliferation, survival, and lactogenic differentiation of MECs, during pregnancy (10)—it is expected to activate multiple downstream mediators that lead to these various cellular responses. Several studies have suggested that the RANK-C/EBPβ and RANK-IKKα-cyclin D1 pathways might activate the expression of milk genes and proliferation, respectively, of MECs (7, 18). However, the signaling pathway responsible for survival and lactogenic differentiation of MECs was unknown prior to this study. Here, we showed that the RANK-Id2 pathway is responsible for cellular survival and lactogenic differentiation, but not proliferation, through the nuclear retention of Id2. While the forced expression of wild-type Id2 did not rescue defective mammary gland development in *RANKL*$^{-/-}$ mice, increased apoptosis and defective lactogenic differentiation in these mice were rescued by the forced nuclear expression of mutant Id2^{S5A}, which cannot be phosphorylated by RANK signaling. Thus, phosphorylation of Id2 at Ser-5 is required for the nuclear retention of Id2 by preventing nuclear export via CRM1/exportin, and it is the nuclear retention of Id2 itself rather than the phosphorylated serine residue that inhibits apoptosis and drives lactogenic differentiation of MECs during pregnancy.

While the forced expression of NLS-Id2^{S5A} induced both survival and lactogenic differentiation, it did not increase the cellular proliferation of MECs in lactating *RANKL*$^{-/-}$ mice. However, we cannot exclude the possibility that RANK-Id2 or unknown upstream Id2 signaling is involved in the cellular proliferation of MECs during pregnancy. Because both *RANKL*$^{-/-}$ and *Id2*$^{-/-}$ mice exhibited impaired proliferation of MECs, the RANK-Id2 pathway might work cooperatively with the RANK-IKKα-cyclin D1 pathway or another signaling pathway triggered by RANK activation, such as IKK, JNK, p38 MAPK, ERK, or unknown mediators (4).

Recent studies suggested that RANKL is one of the paracrine effectors of progesterone-mediated proliferation of MaSC during the reproductive cycle and breast cancer (2, 11, 17, 36). Joshi et al. showed that RANKL is elevated several thousandfold exclusively in sorted luminal cells by progesterone treatment and that the surge in RANK expression in MaSC-enriched basal cells is due to progesterone treatment (17). Indeed, cyclin D1 was the strongest candidate for the RANK downstream effector for progesterone signaling, instead of cyclin D2, in MaSC-enriched basal cells, because several studies suggested that cyclin D1 induces progesterone and/or RANK-mediated MEC proliferation during pregnancy (3, 7). However, the expression of cyclin D1 is not increased in MaSC-enriched basal cells. Recent studies suggested that cyclin D2 and Id2 are the candidates for RANK downstream effector for progesterone signaling, as an increase of cyclin D2 and Id2 expression by progesterone was shown in MaSC-enriched basal cells (2, 17). It can be suggested that the signaling mechanism of proliferation for MaSC homeostasis during the normal estrus cycle might be different from that for luminal cells during pregnancy. Therefore, the question remains whether the nuclear localization and Ser-5 phosphorylation of Id2 are induced by RANK signaling in MaSC-enriched basal cells.

In this study, we focused on RANKL-RANK signaling for proliferation, survival, and lactogenic differentiation of mammary luminal epithelial cells during mammary gland development. We showed that RANK signaling-mediated nuclear retention of Id2 is sufficient for survival and lactogenic differentiation, but not proliferation, of MECs.

ACKNOWLEDGMENTS

We thank the members of Y.-Y.K.'s laboratory for discussions, J. Lee and H. S. Hwang for technical support, I. Ryu in S. K. Jang's laboratory (POSTECH) for teaching affinity purification for p-Id2 (Ser5) antibody, and R. James Turner for kind provision of material.

This research was supported by grants from the National R&D Program for Cancer Control, Ministry of Health and Welfare, Republic of Korea (0920310); the Korea Science and Engineering Foundation from the Korean government (MOST) (2009-0084056); a National Research Foundation of Korea (NRF) grant funded by the Korean Government (MEST) (NRF-M1AXA002-2010-0029780); and the Basic Science Research Program through the National Research Foundation of Korea (2009-0079371).

REFERENCES

1. **Anderson, D. M., et al.** 1997. A homologue of the TNF receptor and its ligand enhance T-cell growth and dendritic-cell function. Nature **390:**175–179.
2. **Asselin-Labat, M. L., et al.** 2010. Control of mammary stem cell function by steroid hormone signalling. Nature **465:**798–802.
3. **Beleut, M., et al.** 2010. Two distinct mechanisms underlie progesterone-induced proliferation in the mammary gland. Proc. Natl. Acad. Sci. U. S. A. **107:**2989–2994.
4. **Boyle, W. J., W. S. Simonet, and D. L. Lacey.** 2003. Osteoclast differentiation and activation. Nature **423:**337–342.
5. **Brisken, C.** 2002. Hormonal control of alveolar development and its implications for breast carcinogenesis. J. Mammary Gland Biol. Neoplasia **7:**39–48.
6. **Brisken, C., et al.** 2002. IGF-2 is a mediator of prolactin-induced morphogenesis in the breast. Dev. Cell **3:**877–887.
7. **Cao, Y., et al.** 2001. IKKalpha provides an essential link between RANK signaling and cyclin D1 expression during mammary gland development. Cell **107:**763–775.

8. **Cartwright, P., and K. Helin.** 2000. Nucleocytoplasmic shuttling of transcription factors. Cell. Mol. Life Sci. **57:**1193–1206.
9. **Fabbro, M., and B. R. Henderson.** 2003. Regulation of tumor suppressors by nuclear-cytoplasmic shuttling. Exp. Cell Res. **282:**59–69.
10. **Fata, J. E., et al.** 2000. The osteoclast differentiation factor osteoprotegerin-ligand is essential for mammary gland development. Cell **103:**41–50.
11. **Gonzalez-Suarez, E., et al.** 2010. RANK ligand mediates progestin-induced mammary epithelial proliferation and carcinogenesis. Nature **468:**103–107.
12. **Hara, E., M. Hall, and G. Peters.** 1997. Cdk2-dependent phosphorylation of Id2 modulates activity of E2A-related transcription factors. EMBO J. **16:** 332–342.
13. **Hennighausen, L., and G. W. Robinson.** 2001. Signaling pathways in mammary gland development. Dev. Cell **1:**467–475.
14. **Hennighausen, L., and G. W. Robinson.** 1998. Think globally, act locally: the making of a mouse mammary gland. Genes Dev. **12:**449–455.
15. **Indra, A. K., et al.** 1999. Temporally-controlled site-specific mutagenesis in the basal layer of the epidermis: comparison of the recombinase activity of the tamoxifen-inducible Cre-ER(T) and Cre-ER(T2) recombinases. Nucleic Acids Res. **27:**4324–4327.
16. **Jones, D. H., et al.** 2006. Regulation of cancer cell migration and bone metastasis by RANKL. Nature **440:**692–696.
17. **Joshi, P. A., et al.** 2010. Progesterone induces adult mammary stem cell expansion. Nature **465:**803–807.
18. **Kim, H. J., M. J. Yoon, J. Lee, J. M. Penninger, and Y. Y. Kong.** 2002. Osteoprotegerin ligand induces beta-casein gene expression through the transcription factor CCAAT/enhancer-binding protein beta. J. Biol. Chem. **277:**5339–5344.
19. **Kim, N. S., et al.** 2006. Receptor activator of NF-kappaB ligand regulates the proliferation of mammary epithelial cells via Id2. Mol. Cell. Biol. **26:**1002–1013.
20. **Kong, Y. Y., et al.** 1999. OPGL is a key regulator of osteoclastogenesis, lymphocyte development and lymph-node organogenesis. Nature **397:**315–323.
21. **Kurooka, H., and Y. Yokota.** 2005. Nucleo-cytoplasmic shuttling of Id2, a negative regulator of basic helix-loop-helix transcription factors. J. Biol. Chem. **280:**4313–4320.
22. **Lacey, D. L., et al.** 1998. Osteoprotegerin ligand is a cytokine that regulates osteoclast differentiation and activation. Cell **93:**165–176.
23. **Lasorella, A., and A. Iavarone.** 2006. The protein ENH is a cytoplasmic sequestration factor for Id2 in normal and tumor cells from the nervous system. Proc. Natl. Acad. Sci. U. S. A. **103:**4976–4981.
24. **Lasorella, A., et al.** 2006. Degradation of Id2 by the anaphase-promoting complex couples cell cycle exit and axonal growth. Nature **442:**471–474.
25. **Li, X., et al.** 2005. Polycystin-1 and polycystin-2 regulate the cell cycle through the helix-loop-helix inhibitor Id2. Nat. Cell Biol. **7:**1202–1212.
26. **Lombardi, M., et al.** 2008. Hormone-dependent nuclear export of estradiol receptor and DNA synthesis in breast cancer cells. J. Cell Biol. **182:**327–340.
27. **Matsumura, M. E., D. R. Lobe, and C. A. McNamara.** 2002. Contribution of the helix-loop-helix factor Id2 to regulation of vascular smooth muscle cell proliferation. J. Biol. Chem. **277:**7293–7297.
28. **Miyoshi, K., et al.** 2002. Mammary epithelial cells are not able to undergo pregnancy-dependent differentiation in the absence of the helix-loop-helix inhibitor Id2. Mol. Endocrinol. **16:**2892–2901.
29. **Miyoshi, K., et al.** 2001. Signal transducer and activator of transcription (Stat) 5 controls the proliferation and differentiation of mammary alveolar epithelium. J. Cell Biol. **155:**531–542.
30. **Mori, S., S. I. Nishikawa, and Y. Yokota.** 2000. Lactation defect in mice lacking the helix-loop-helix inhibitor Id2. EMBO J. **19:**5772–5781.
31. **Mulac-Jericevic, B., J. P. Lydon, F. J. DeMayo, and O. M. Conneely.** 2003. Defective mammary gland morphogenesis in mice lacking the progesterone receptor B isoform. Proc. Natl. Acad. Sci. U. S. A. **100:**9744–9749.
32. **Norton, J. D., R. W. Deed, G. Craggs, and F. Sablitzky.** 1998. Id helix-loop-helix proteins in cell growth and differentiation. Trends Cell Biol. **8:**58–65.
33. **Rane, M. J., et al.** 2001. p38 kinase-dependent MAPKAPK-2 activation functions as 3-phosphoinositide-dependent kinase-2 for Akt in human neutrophils. J. Biol. Chem. **276:**3517–3523.
34. **Romieu-Mourez, R., et al.** 2003. Mouse mammary tumor virus c-rel transgenic mice develop mammary tumors. Mol. Cell. Biol. **23:**5738–5754.
35. **Samanta, J., and J. A. Kessler.** 2004. Interactions between ID and OLIG proteins mediate the inhibitory effects of BMP4 on oligodendroglial differentiation. Development **131:**4131–4142.
36. **Schramek, D., et al.** 2010. Osteoclast differentiation factor RANKL controls development of progestin-driven mammary cancer. Nature **468:**98–102.
37. **Shillingford, J. M., K. Miyoshi, M. Flagella, G. E. Shull, and L. Hennighausen.** 2002. Mouse mammary epithelial cells express the Na-K-Cl cotransporter, NKCC1: characterization, localization, and involvement in ductal development and morphogenesis. Mol. Endocrinol. **16:**1309–1321.
38. **Sinn, E., et al.** 1987. Coexpression of MMTV/v-Ha-ras and MMTV/c-myc genes in transgenic mice: synergistic action of oncogenes in vivo. Cell **49:** 465–475.
39. **Smith, J. M., and P. A. Koopman.** 2004. The ins and outs of transcriptional control: nucleocytoplasmic shuttling in development and disease. Trends Genet. **20:**4–8.
40. **Srivastava, S., et al.** 2003. Receptor activator of NF-kappaB ligand induction via Jak2 and Stat5a in mammary epithelial cells. J. Biol. Chem. **278:**46171–46178.
41. **Tu, X., R. Baffa, S. Luke, M. Prisco, and R. Baserga.** 2003. Intracellular redistribution of nuclear and nucleolar proteins during differentiation of 32D murine hemopoietic cells. Exp. Cell Res. **288:**119–130.
42. **Wang, S., A. Sdrulla, J. E. Johnson, Y. Yokota, and B. A. Barres.** 2001. A role for the helix-loop-helix protein Id2 in the control of oligodendrocyte development. Neuron **29:**603–614.
43. **Yokota, Y., et al.** 1999. Development of peripheral lymphoid organs and natural killer cells depends on the helix-loop-helix inhibitor Id2. Nature **397:**702–706.